Title: CDT without preferred foliation

Date: May 30, 2013 02:30 PM

URL: http://pirsa.org/13050082

Abstract: Causal dynamical triangulations (CDT) define a nonperturbative path integral for quantum gravity as a sum over triangulations. Causality is enforced on the kinematical level by means of a preferred
foliation.

In this talk I present a new model of dynamical triangulations based on Lorentzian building blocks, where the triangulations in general do not have such a preferred foliation. The essential ingredients of the new model are a local causality constraint and a consistency condition on the global flow of time. After a compact review on CDT I discuss the theoretical aspects of the new model in 1+1 and 2+1 dimensions, followed by a presentation of numerical results in 2+1 dimensions. These results show that the new model and CDT have similar long-distance properties in 2+1 dimensions.

CDT without preferred foliation

S. Jordan[1] R. Loll[1]

[1] Radboud University, Nijmegen, The Netherlands

Perimeter Institute, May 30th, 2013

About this talk

Causal dynamical triangulations (CDT) are a proposal to define a nonperturbative path integral of gravity as a sum over triangulations.

CDT implements causality using a preferred foliation.

In this talk we discuss the following question:

Is the preferred foliation necessary to define a DT model consistent with cosmological observations?

A path integral of gravity

The idea of a superposition of curved spacetimes can be mathematically expressed using a pure gravity path integral:

$$Z = \int_{\text{geometries}} \mathcal{D}[g] \exp(iS_{EH}[[g]])$$

- This formal expression can be regularized in a coordinate free way by introducing a simplicial complex. The sum is then effectively over equivalence classes of metrics.
- S_{EH} is the Einstein-Hilbert action.
- Which geometries should be summed over?

Causal Dynamical Triangulations (CDT)

CDT proposes to sum over causal triangulations, which are Lorentzian triangulations with a foliated structure. Each leaf of the foliation is labeled by a time parameter.

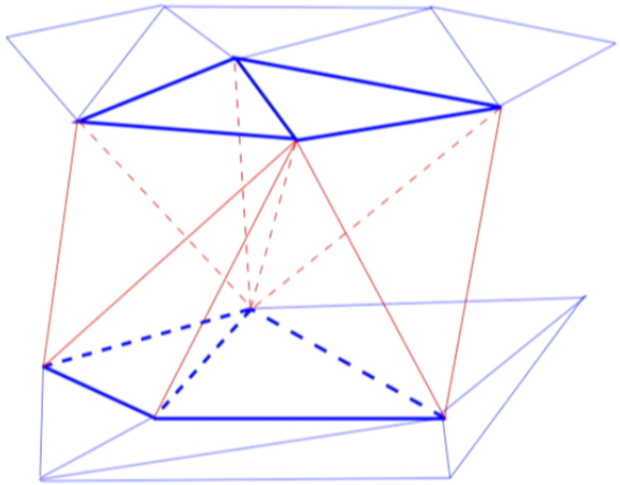

Blue links are spacelike

Red links are timelike

The Regge action

The discretized and Wick-rotated version of the Einstein-Hilbert action is called the Euclidean Regge action. In 3+1 dimensions it can be written in the form

$$S^{\text{eucl}}_{\text{Regge}} = -(\kappa_0 + 6\Delta)N_0 + \kappa_4 N_4 + \Delta N_4^{(4,1)}$$

with $(\kappa_0, \kappa_4, \Delta) = f(G_{\text{bare}}, \Lambda_{\text{bare}}, \alpha)$.

The asymmetry parameter α is defined by the relation $l_s^2 = -\alpha l_t^2$ where l_s^2 and l_t^2 are the squared lengths of the spacelike and timelike links.

N_0, N_4 and $N_4^{(4,1)}$ are the number of sub-simplices of various types.

The regularized path integral

The CDT prescription allows us to convert the formal expression for the continuum path integral into a form which is suitable to be explored using Monte Carlo simulations:

$$Z(G_{\text{bare}}, \Lambda_{\text{bare}}) = \int_{\text{geometries}} \mathcal{D}[g] \exp(iS_{EH}[[g]])$$

$$\Downarrow$$

$$Z(\kappa_0, \kappa_4, \Delta) = \sum_{T \in \mathcal{T}} \frac{1}{C(T)} \exp(-S^{\text{eucl}}_{\text{Regge}}(T))$$

$\mathcal{T}$ is the space of all foliated triangulations and $1/C(T)$ is a discrete measure.

The CDT phase diagram ($d = 3 + 1$)

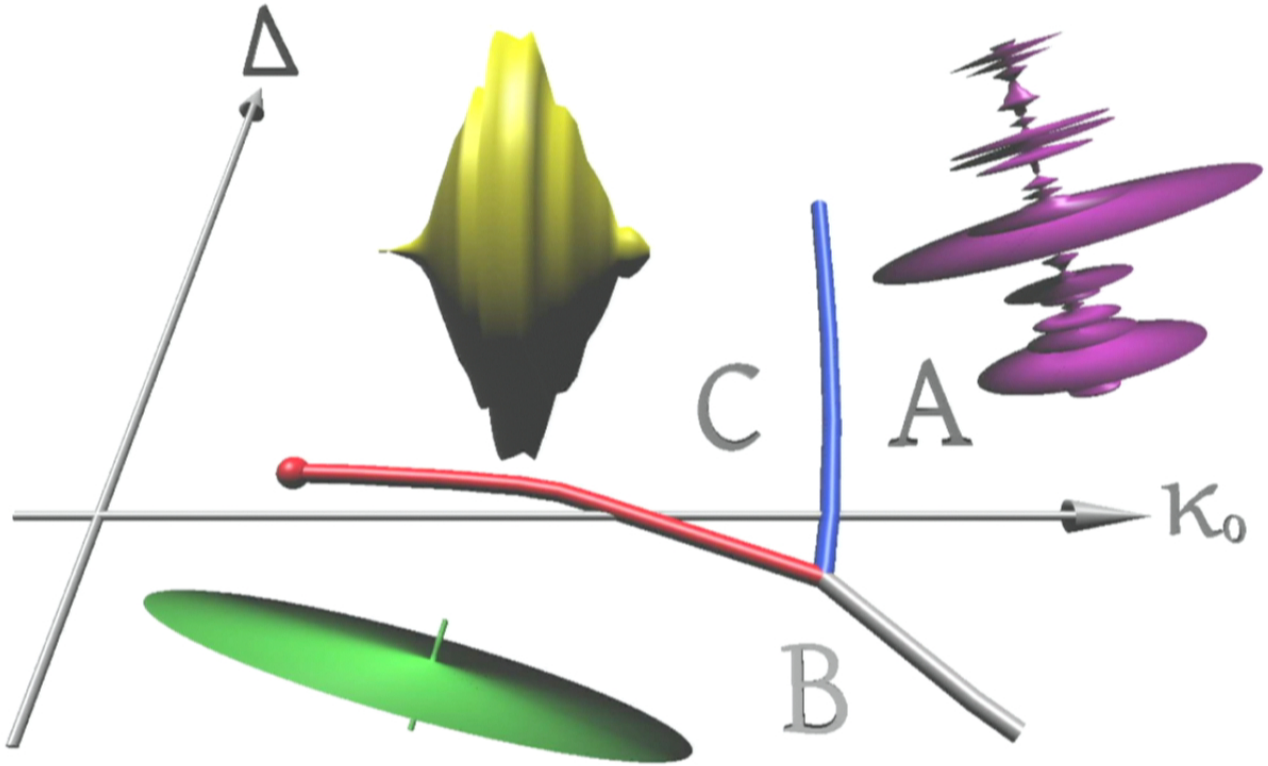

CDT successes in $d = 3 + 1$

- Scale-dependent spectral dimension in phase C, flowing from $d_s = 4$ at low energies to $d_s \approx 2$ at high energies.
- Hausdorff dimension $d_h = 4$ in phase C.
- Volume profile in phase C compatible with Wick-rotated de Sitter spacetime.
- B-C phase transition is second order, thus providing a line of candidate UV fixed points.

CDT successes in $d = 3 + 1$

- Scale-dependent spectral dimension in phase C, flowing from $d_s = 4$ at low energies to $d_s \approx 2$ at high energies.
- Hausdorff dimension $d_h = 4$ in phase C.
- Volume profile in phase C compatible with Wick-rotated de Sitter spacetime.
- B-C phase transition is second order, thus providing a line of candidate UV fixed points.

CDT successes in $d = 3 + 1$

- Scale-dependent spectral dimension in phase C, flowing from $d_s = 4$ at low energies to $d_s \approx 2$ at high energies.
- Hausdorff dimension $d_h = 4$ in phase C.
- Volume profile in phase C compatible with Wick-rotated de Sitter spacetime.
- B-C phase transition is second order, thus providing a line of candidate UV fixed points.

Removing the preferred foliation

The distinguished foliation is an essential new ingredient in CDT compared to the older Euclidean dynamical triangulations.

But is the foliation really necessary to get interesting physics out of a DT model?

To clarify this question we need to build a DT model lying in between Euclidean DT and CDT. In the next part we introduce such a model:

Locally causal dynamical triangulations.

Looking for Lorentzian triangles

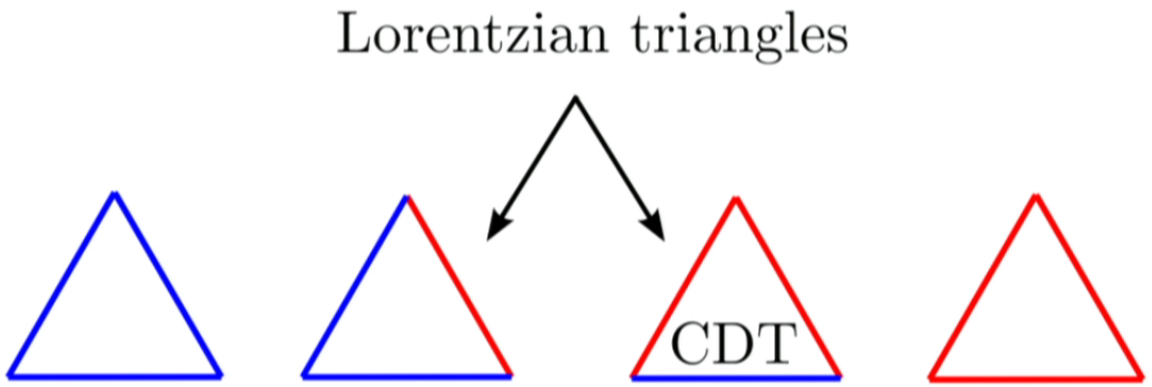

We need flat triangles with Lorentzian signature, where the squared lengths of all links of each type (spacelike and timelike) are equal.

There are two of them, only one of them is used in CDT!

The local causality condition

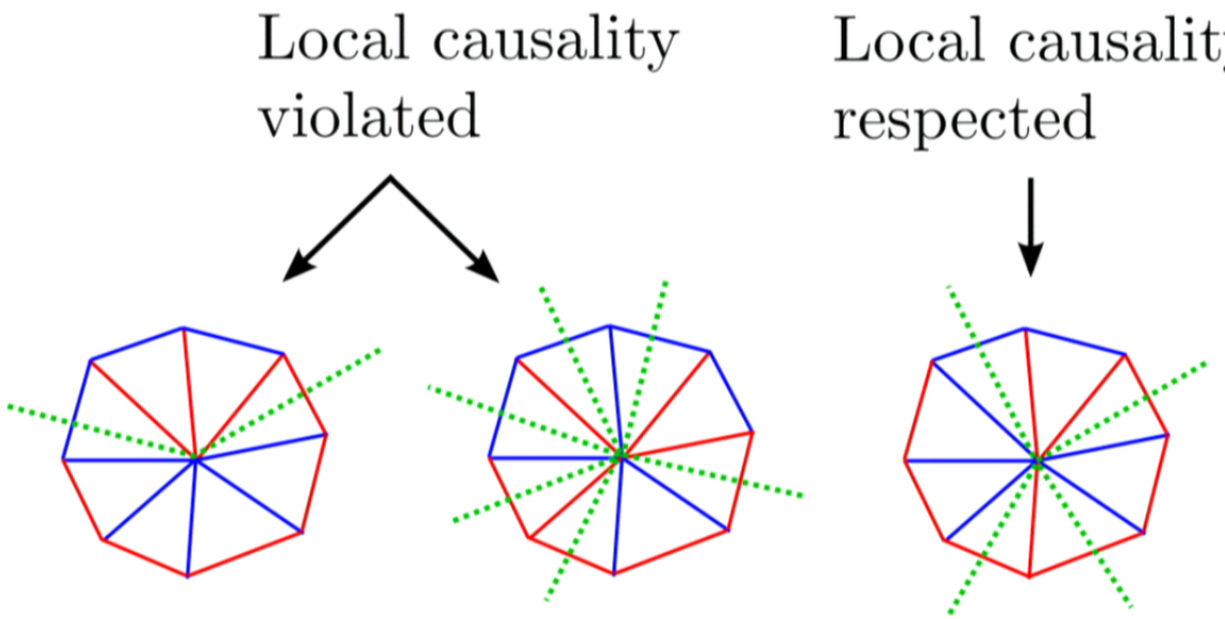

In order to get valid light cones at the vertices, we require that there are exactly four light cone crossings when circling around a vertex.

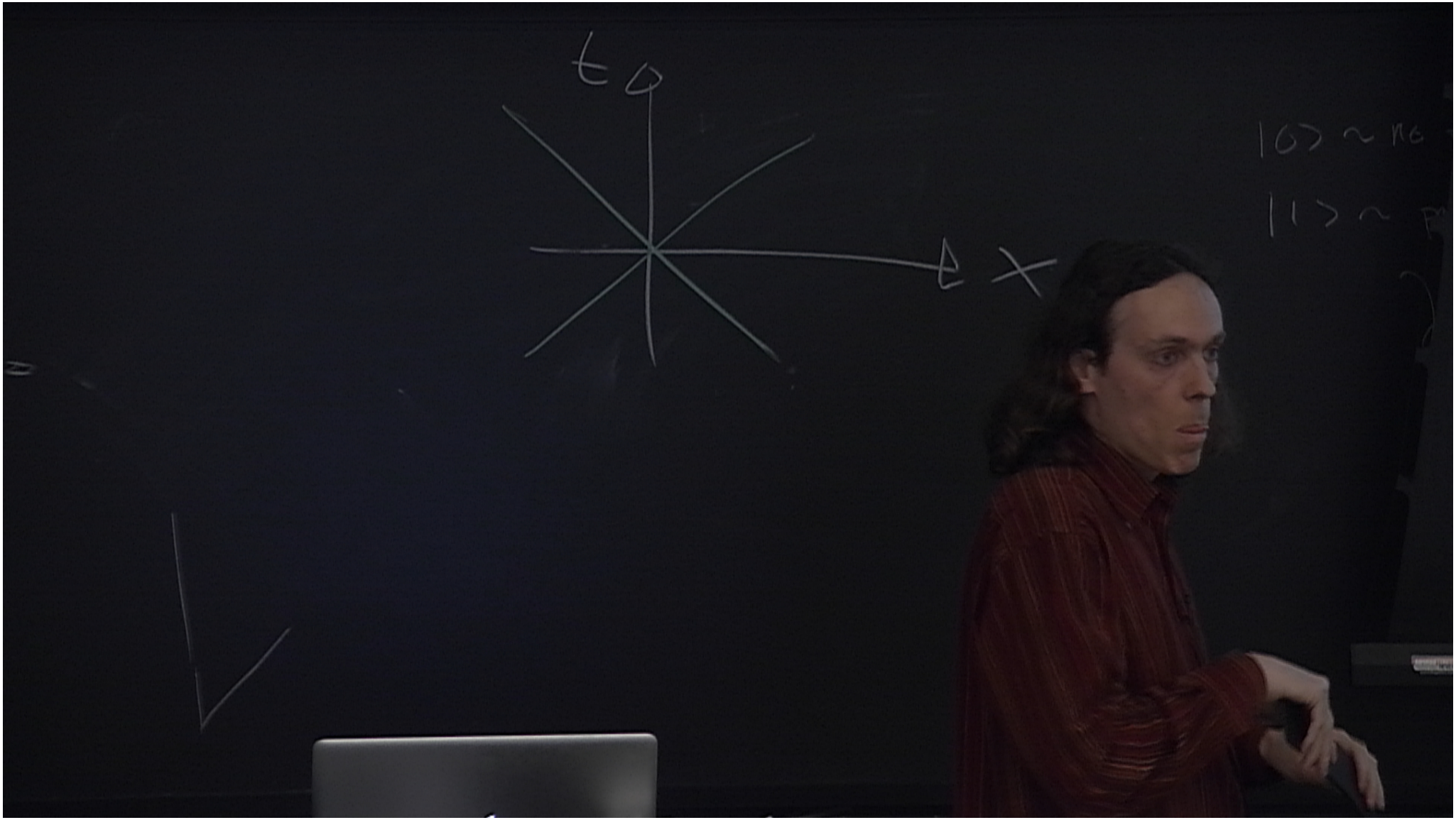
t
x

Time-orienting Lorentzian triangles

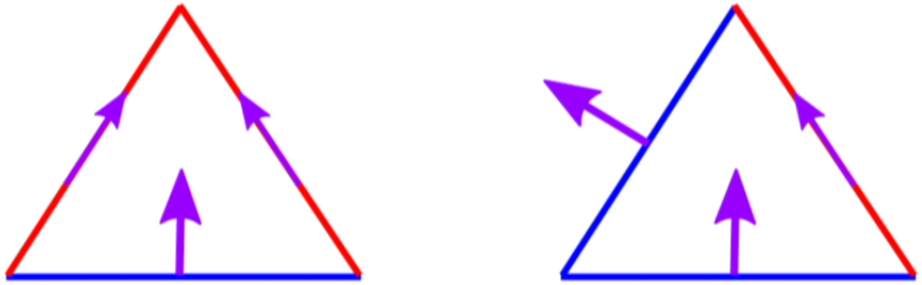

We can assign one of the two possible time-orientations to a Lorentzian triangle, as shown in the figure.

It is clear that the time-orientations of every neighbor triangle is uniquely determined by consistency at the shared link.

Time-orienting Lorentzian triangles

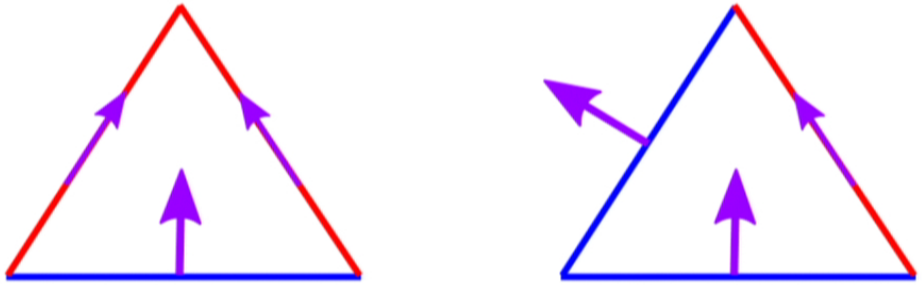

We can assign one of the two possible time-orientations to a Lorentzian triangle, as shown in the figure.

It is clear that the time-orientations of every neighbor triangle is uniquely determined by consistency at the shared link.

Extending the time orientation

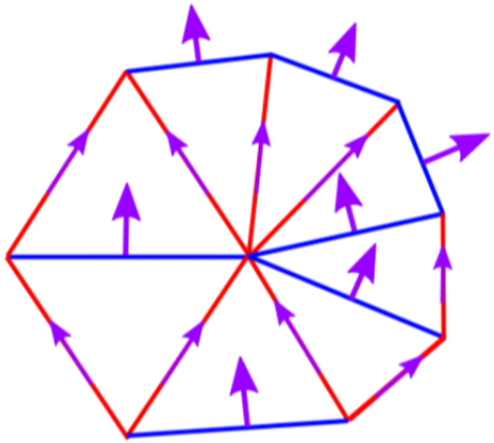

If local causality holds, we can (at least locally) extend the time-orientation.

Depending on the chosen spacetime topology it may not be possible to extend the time-orientation globally. We therefore require that such a global extension always exists.

Kinematical objects in 1+1 dimensions

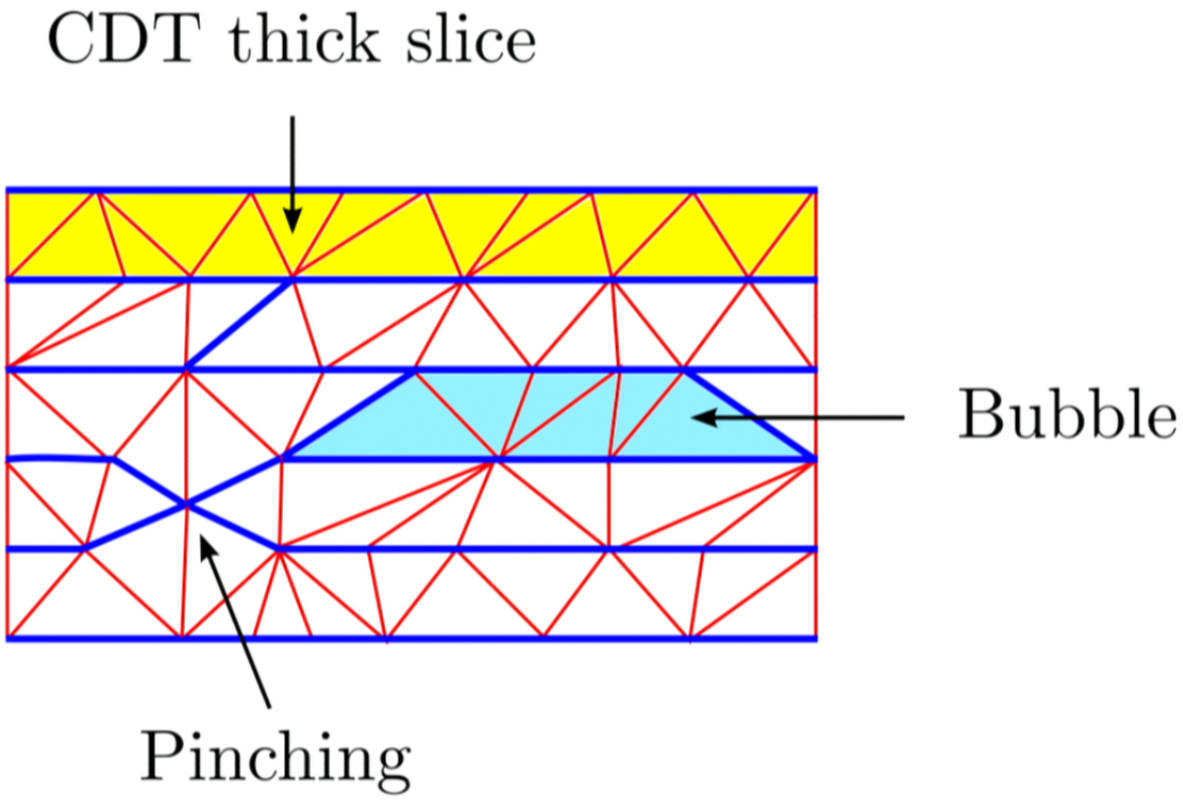

Going up to 2+1 dimensions

After this short introduction into locally causal DT in 1+1 dimensions we will discuss the model in 2+1 dimensions.

Why $d = 2 + 1$?

- Use the 2+1 dimensional model as testing ground to learn how to deal with new problems.
- The numerical implementation of the model is much harder compared to CDT even in 2+1 dimensions. Having a working software for $d = 2 + 1$ would greatly help developing a software for $d = 3 + 1$.
- Experience from CDT indicates that $d = 2 + 1$ can give us valuable hints about what to expect for $d = 3 + 1$.

Lorentzian tetrahedra

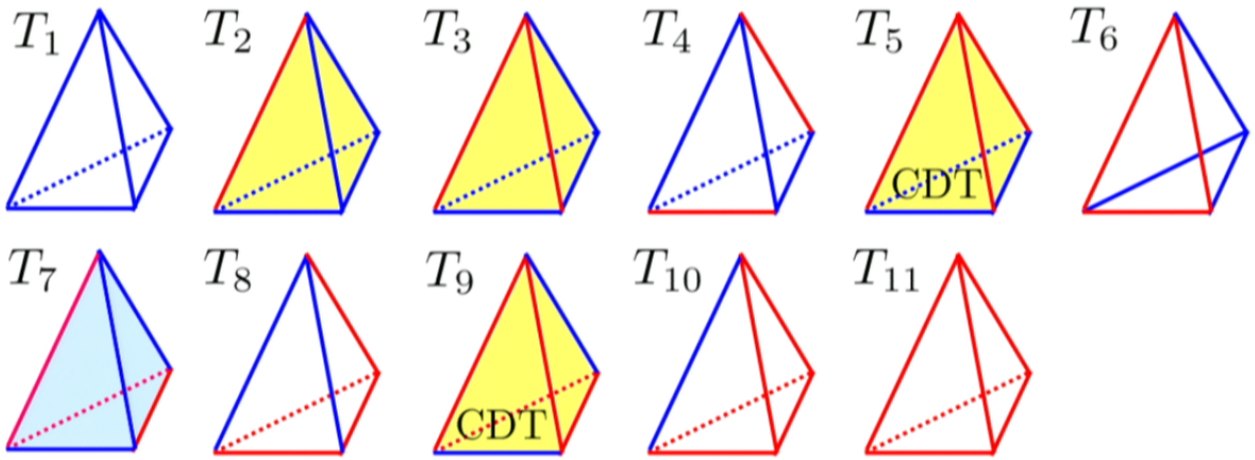

The tetrahedra marked in yellow are Lorentzian. The T_7 tetrahedron is only Lorentzian for $\alpha < 1$ (α is the asymmetry parameter defined by $l_t^2 = -\alpha l_s^2$, where l_s^2 and l_t^2 are the squared lengths of both link types).

The Regge action

We have chosen to work with the discrete Einstein-Hilbert action, also known as the Regge action. The Euclidean version can be brought into the following form:

$$S^{\mathrm{eucl}}_{\mathrm{Regge}} = \widetilde{c}_1 N_0 + \widetilde{c}_2 N_3 + \widetilde{c}_3 N_3^{T_2} + \widetilde{c}_4 N_3^{T_3} + \widetilde{c}_5 N_3^{T_5}.$$
$$\widetilde{c}_i = f_i(G_{\mathrm{bare}}, \Lambda_{\mathrm{bare}}, \alpha)$$

Note that the space of actions spanned by the $\widetilde{c}_i$ couplings is strictly larger than the space of all Regge actions (this was not the case in CDT). We therefore need the explicit expressions $\widetilde{c}_i = f_i(G_{\mathrm{bare}}, \Lambda_{\mathrm{bare}}, \alpha)$.

The choice of topology

CDT uses periodic boundary conditions in time direction and therefore a $\mathcal{T} \times S^1$ topology.

Due to technical difficulties with periodic boundary conditions we decided to use the 3-sphere topology. We place a source and sink of (Euclidean) time at the two poles.

This is also motivated by the fact that in the de-Sitter phase of 2+1-dimensional CDT with $\mathcal{T} = S^2$ the topology effectively changes from $S^2 \times S^1$ to S^3.

Exploring the phase diagram

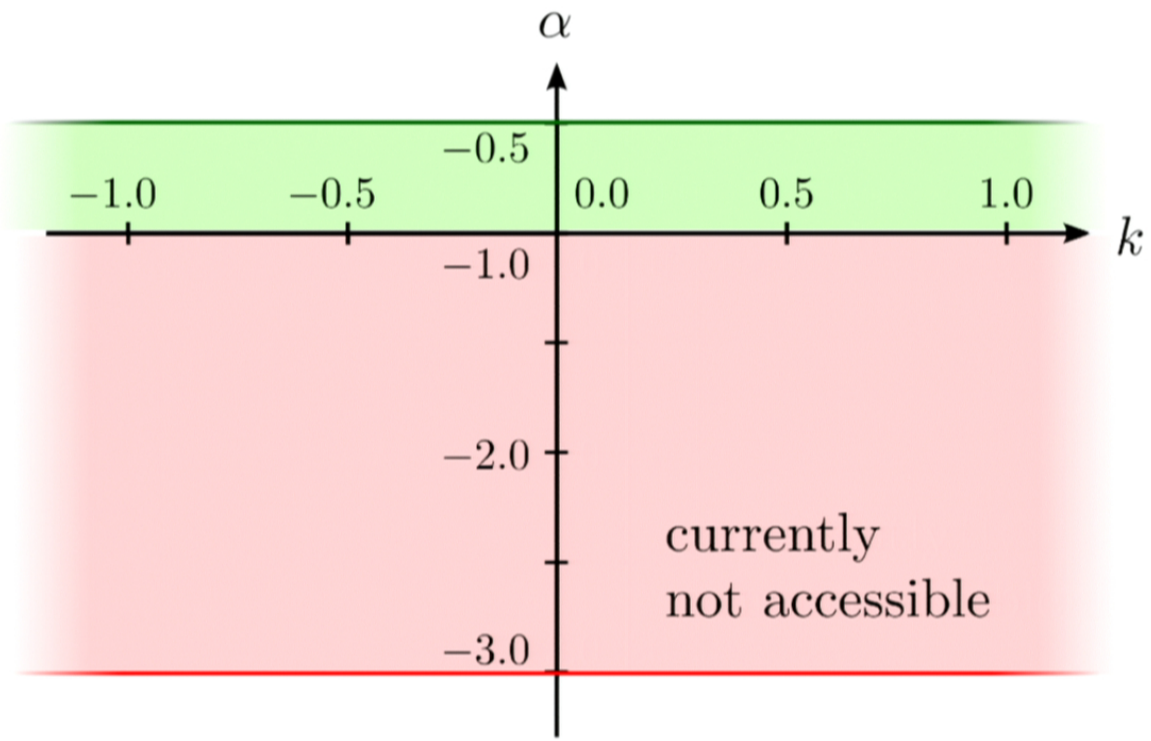

In the following we will numerically explore the k-axis ($k \sim 1/G_{\text{bare}}$) and the α-axis in the region $-1 < \alpha < 1/2$.

Tetrahedron statistics on the k-axis

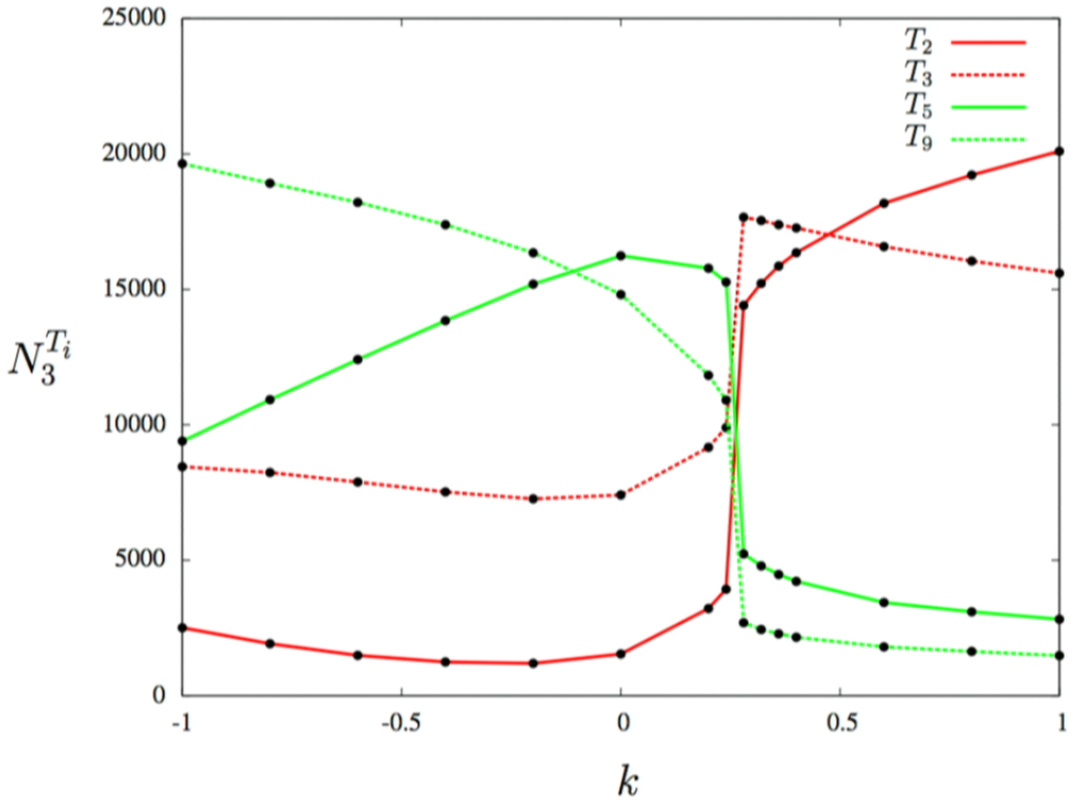

We see the clear sign of a phase transition at $k \approx 0.25$.

Tetrahedron statistics on the k-axis

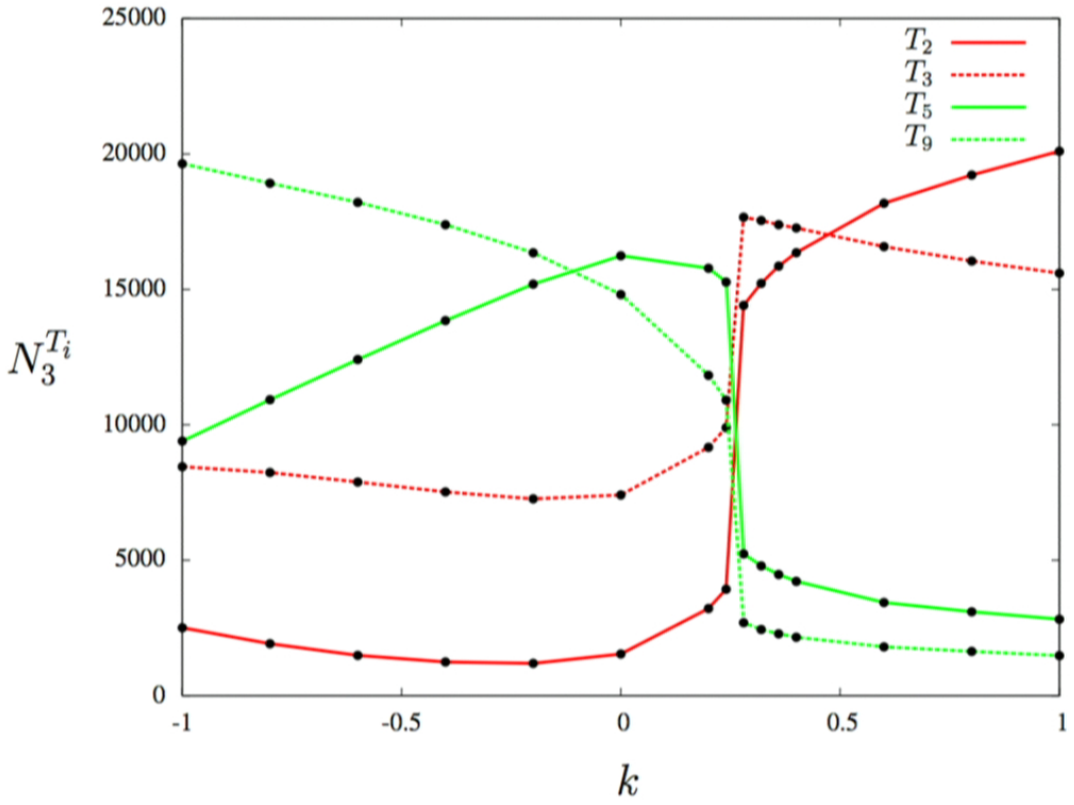

We see the clear sign of a phase transition at $k \approx 0.25$.

Tetrahedron statistics on the α-axis

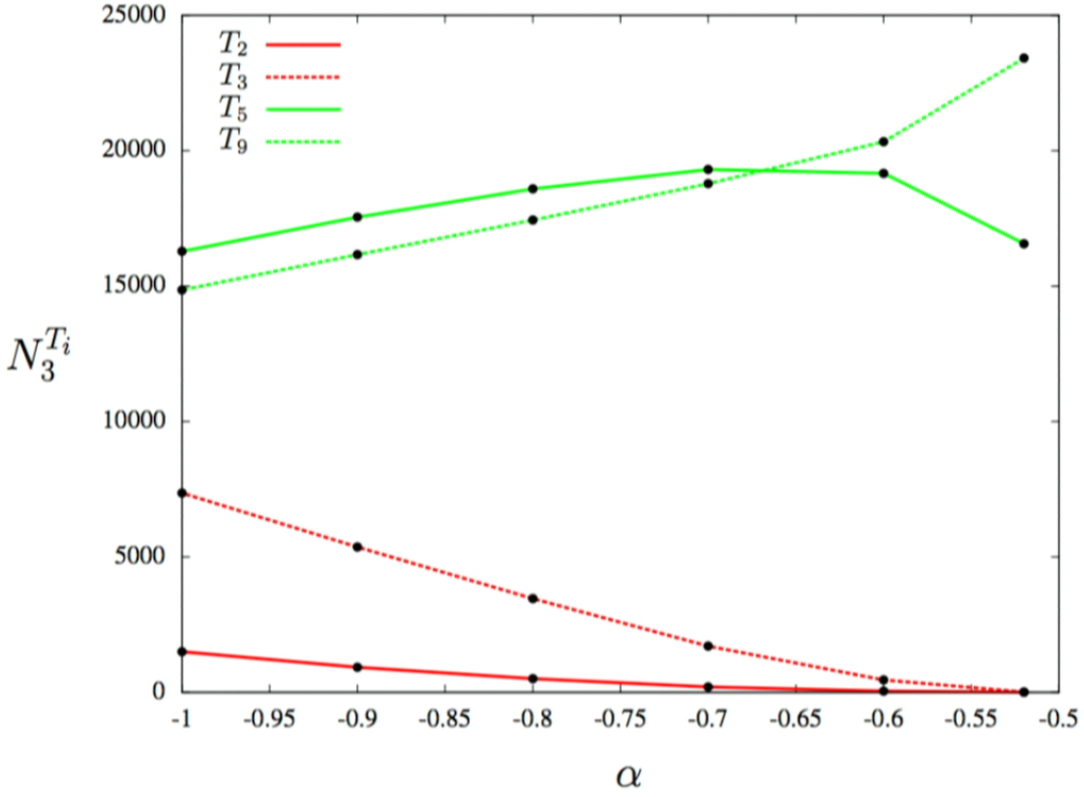

CDT emerges at the phase boundary at $\alpha = 1/2$!

Defining a time coordinate

We are interested in measuring observables which measure some quantity in function of a time variable.

Unlike in CDT there is no canonical time variable in the new model. We introduce a new time variable as follows:

For every vertex we measure the average distance to each pole of the 3-sphere and define the time of the vertex to be the difference of both values.

For foliated triangulations this time variable reduces to the canonical time of CDT.

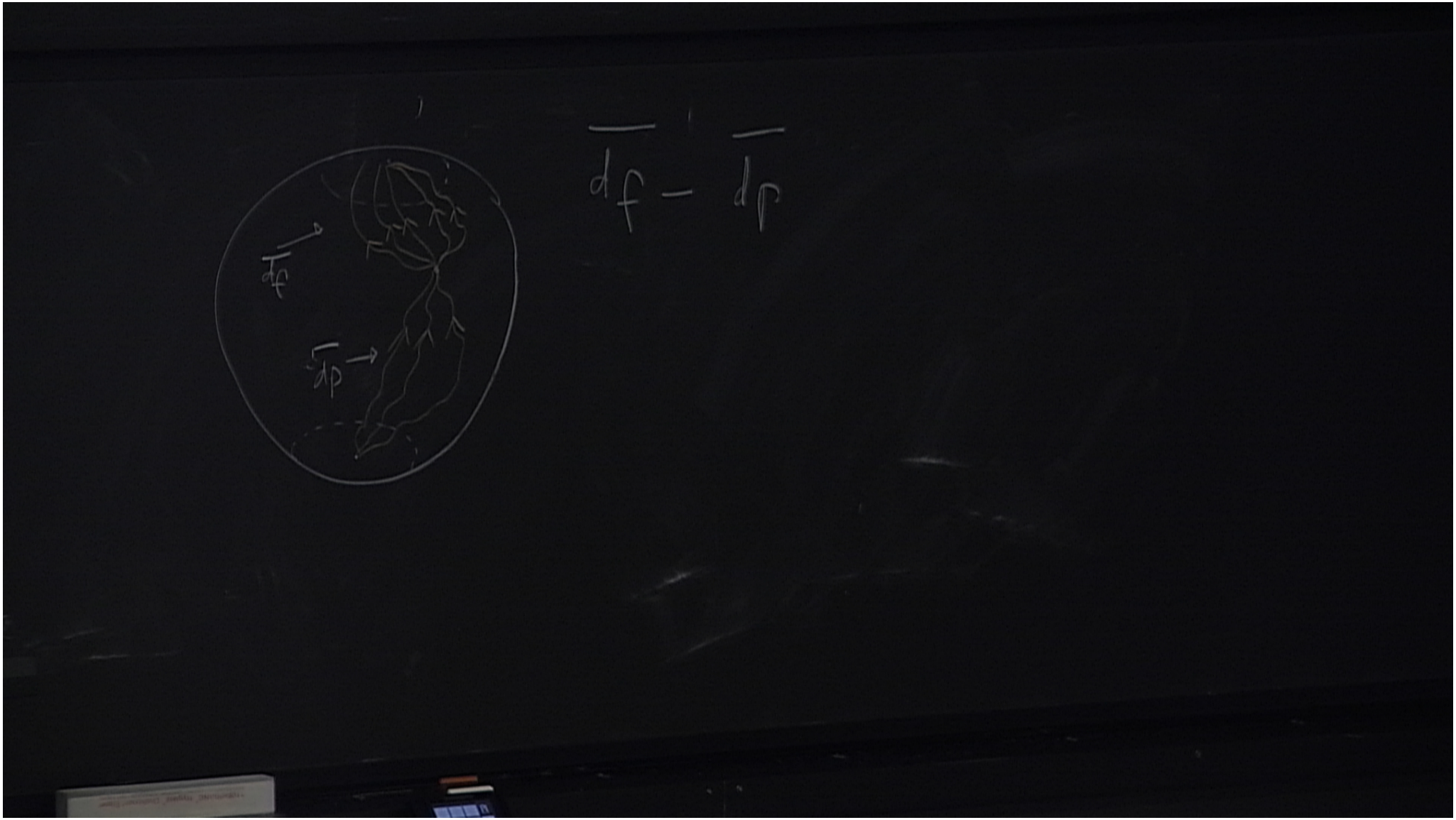
$\vec{d_f}$
$\vec{d_p}$
$\vec{d_f} - \vec{d_p}$

A “foliation observable”

Once every vertex is assigned a time we can immediately assign a time to every tetrahedron.

Now we count the number of tetrahedra in a time interval $[t, t + \Delta t]$ and produce a histogram. For CDT it shows an alternation pattern, reflecting the foliation:

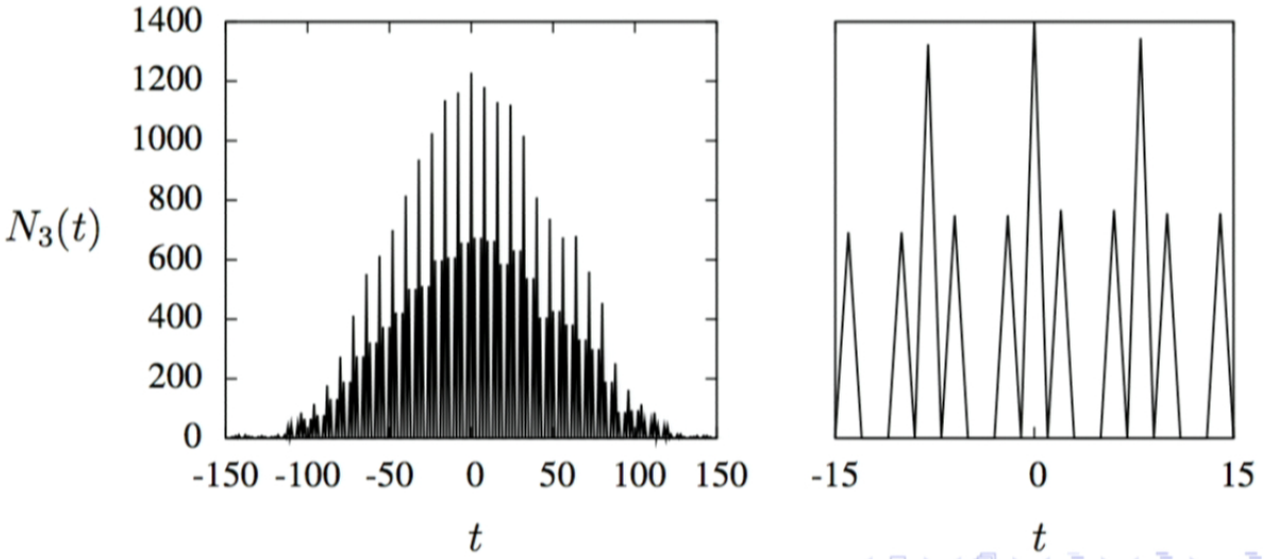

Weakly foliated triangulations

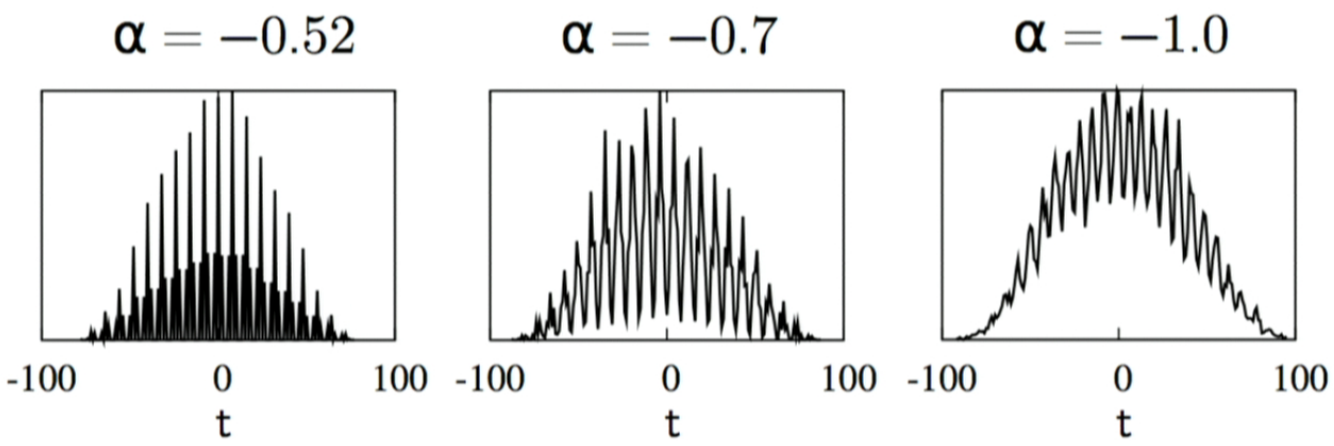

In the new model at $\alpha = -0.52$, close to the "CDT-corner", we find almost the same pattern as for plain CDT.

At $\alpha - 0.7$ and $\alpha = -1.0$ we still see an alternation pattern, indicating the presence of "weakly foliated" triangulations.

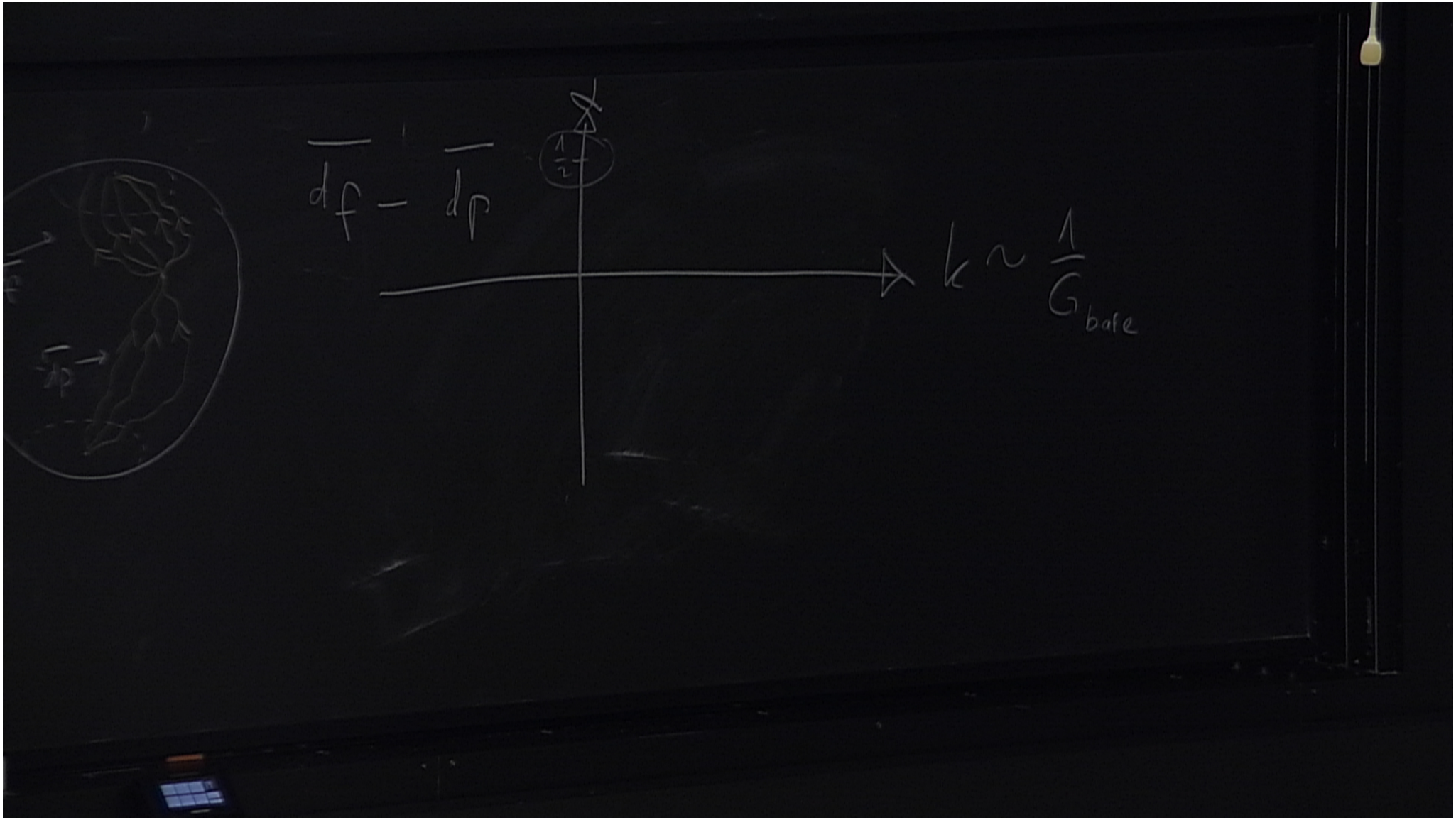
$\bar{d}_f - \bar{d}_p$
$\frac{1}{2}$
$k \sim \frac{1}{G_{bare}}$

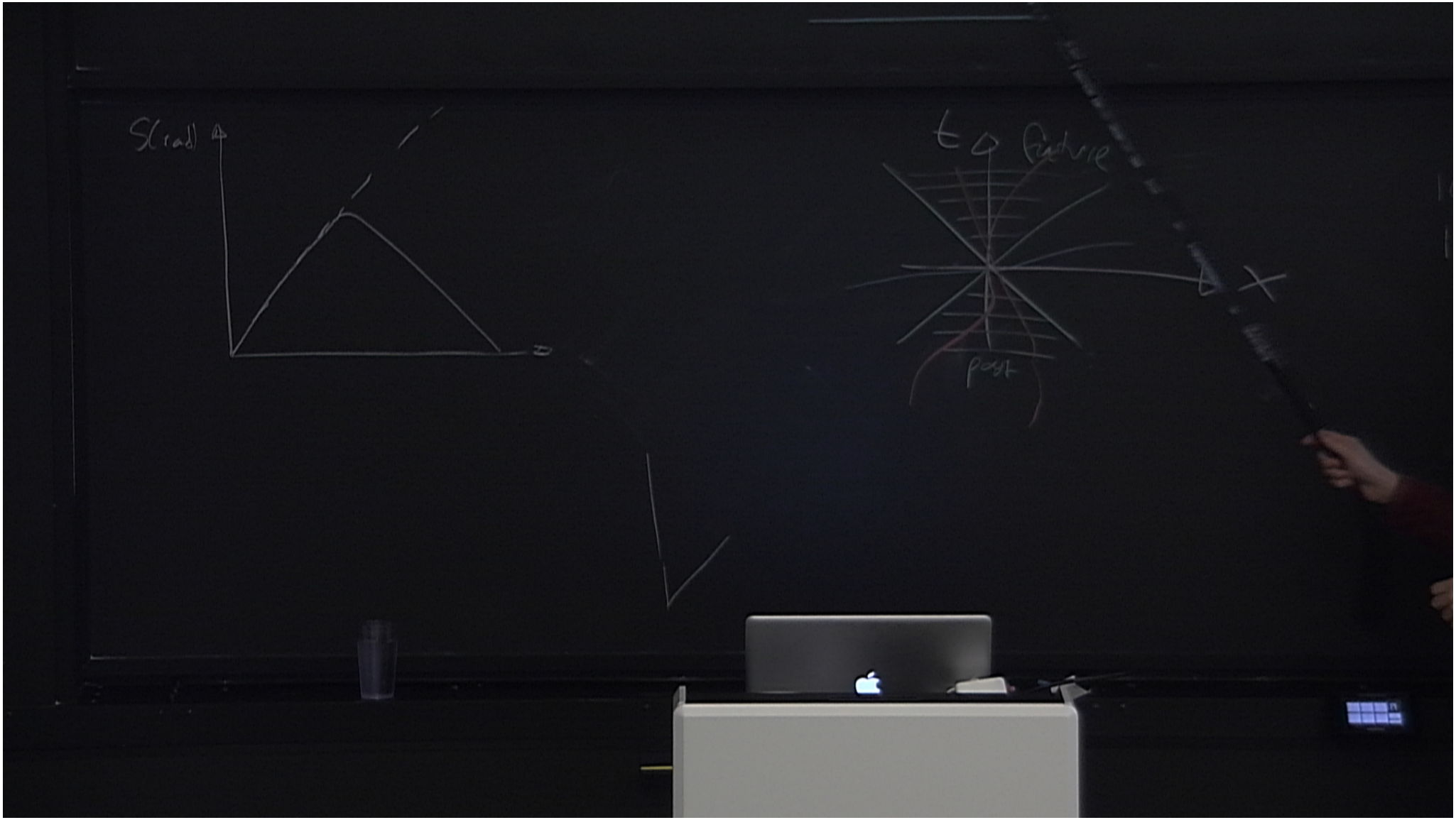
S(rad)
t
Future
Past
x

Spatial slices

In order to study volume profiles, we need to discuss spatial slices first.

In the locally causal DT model, the number of spatial slices can become very large. There are 64 of them in the figure below, one of them highlighted in light blue:

Since we can not enumerate all spatial slices in a triangulation, we use a statistical method to generate a representative subset of all slices.

Spatial slices

In order to study volume profiles, we need to discuss spatial slices first.

In the locally causal DT model, the number of spatial slices can become very large. There are 64 of them in the figure below, one of them highlighted in light blue:

Since we can not enumerate all spatial slices in a triangulation, we use a statistical method to generate a representative subset of all slices.

A single volume profile

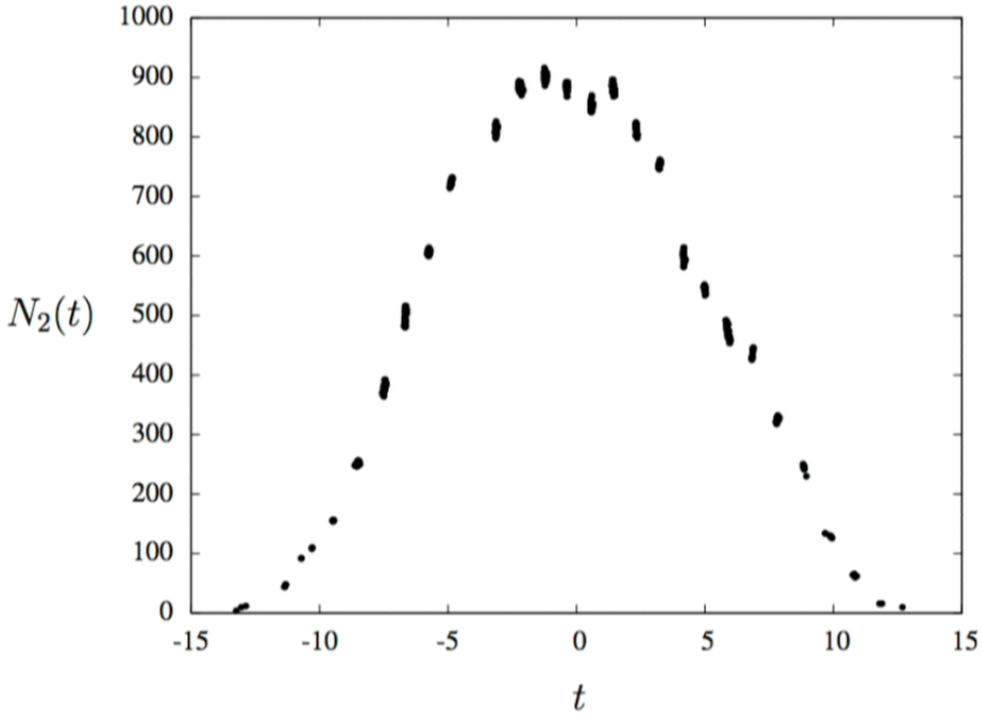

Every dot in the figure is one spatial slice. We see dot clusters and gaps in between. This is also a signature of a weakly foliated triangulation.

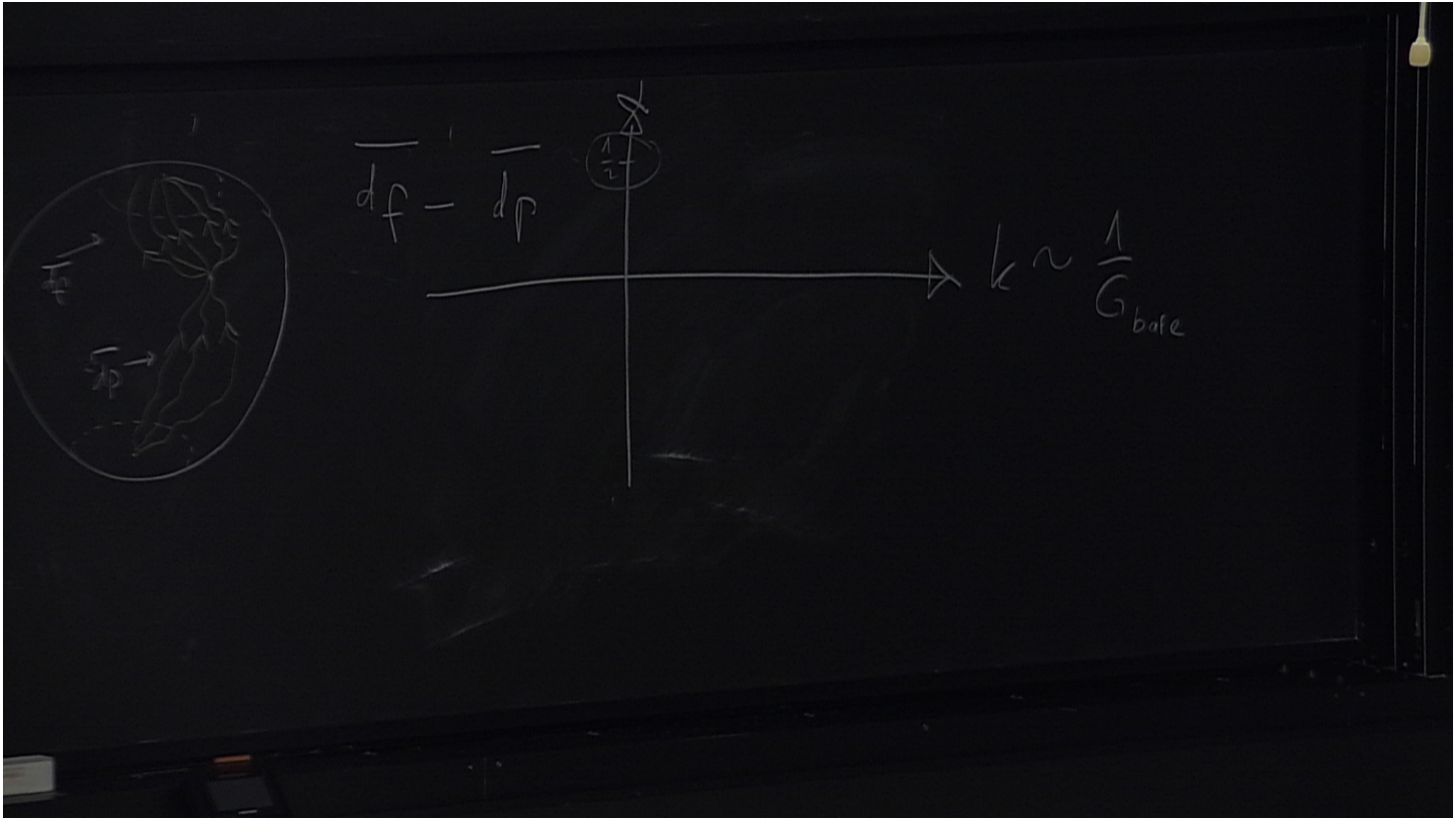
$\bar{d}_f - \bar{d}_p$
$k \sim \frac{1}{G_{bare}}$

Averaging volume profiles

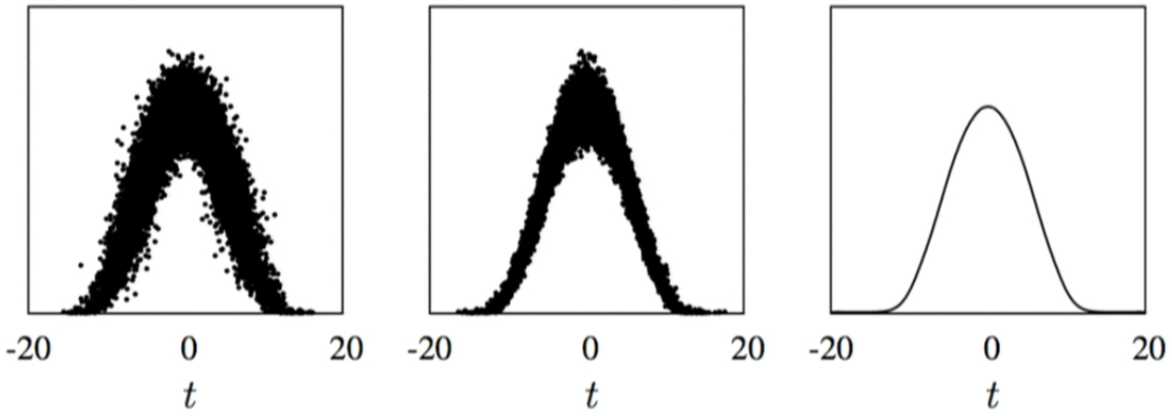

We determine an average volume profile using a sophisticated averaging algorithm.

We find that the new model has a phase of extended geometries with a characteric blob-shaped volume profile!

Finite-size scaling of volume profiles

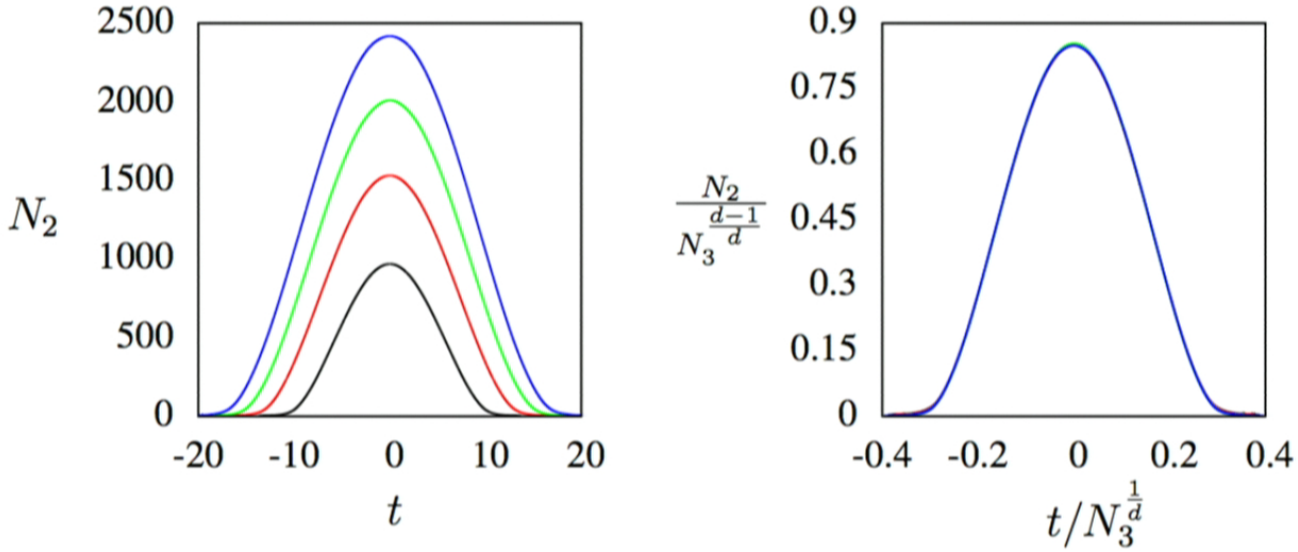

We have measured average volume profiles with four different system sizes, at various locations in the phase diagram.

In the figure, the best overlap is achieved with a global Hausdorff dimension $d = 2.91$.

Finite-size scaling of volume profiles

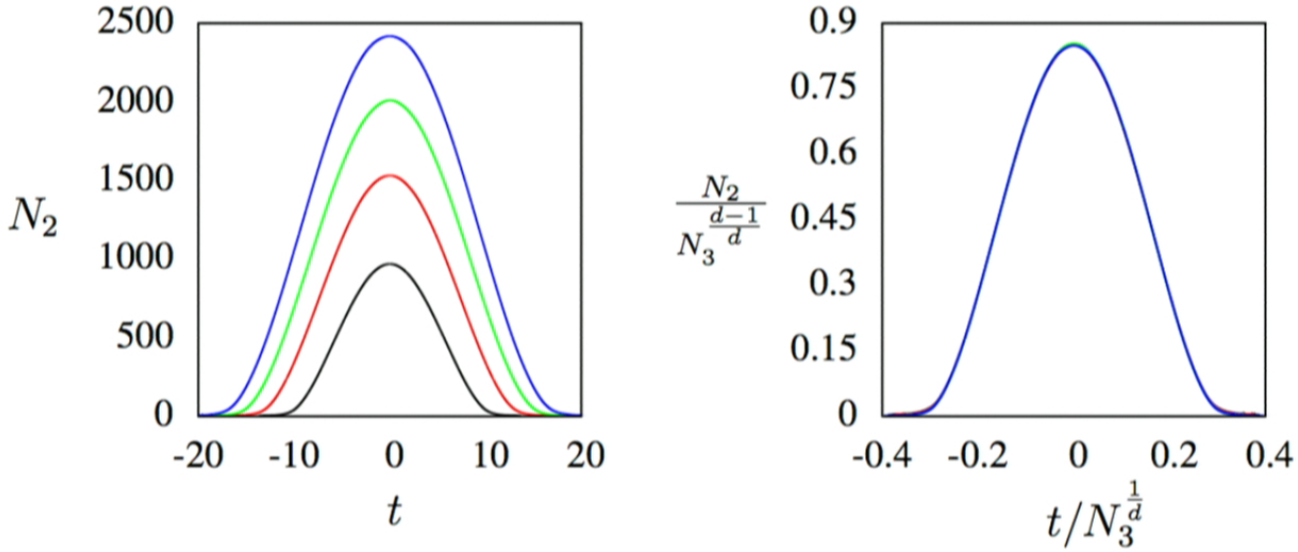

We have measured average volume profiles with four different system sizes, at various locations in the phase diagram.

In the figure, the best overlap is achieved with a global Hausdorff dimension $d = 2.91$.

Finite-size scaling of volume profiles

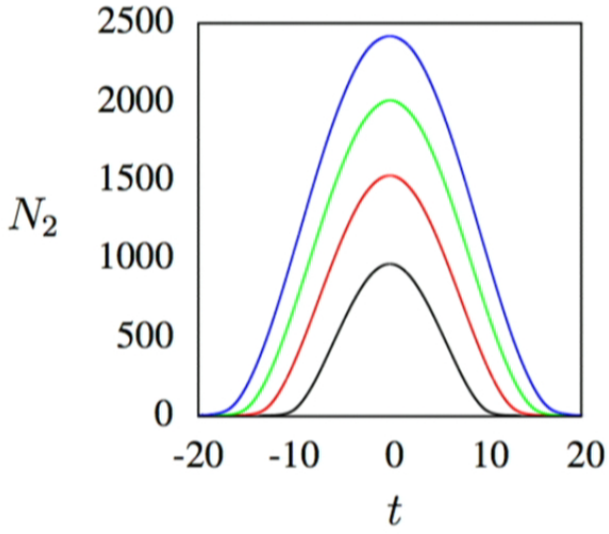

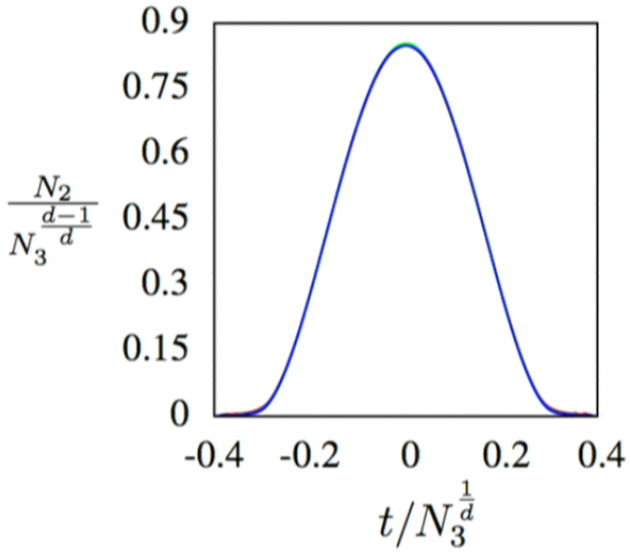

We have measured average volume profiles with four different system sizes, at various locations in the phase diagram.

In the figure, the best overlap is achieved with a global Hausdorff dimension $d = 2.91$.

The global Hausdorff dimension

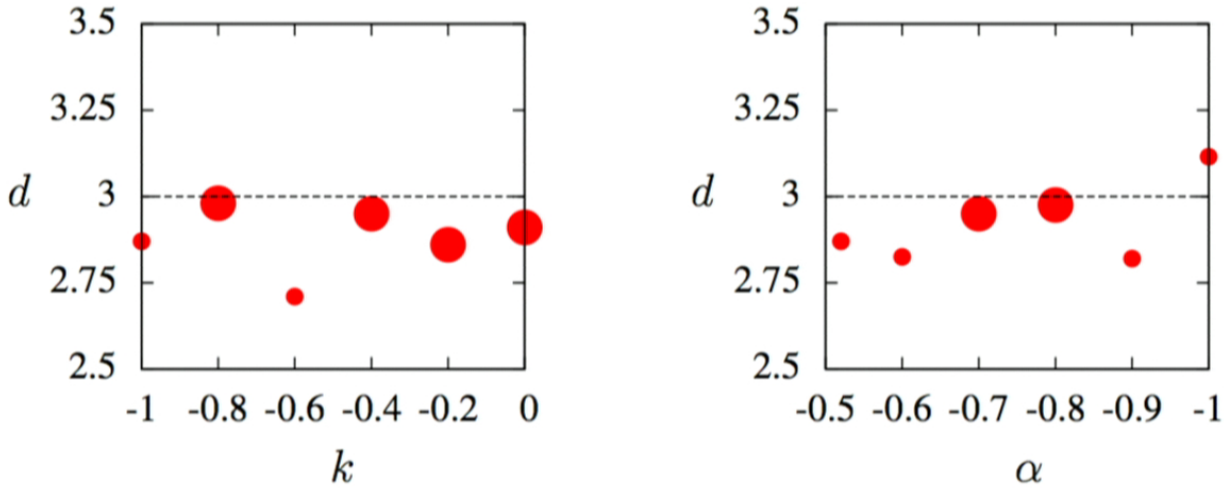

Further measurements on the k-axis and the α-axis support the $d = 3$ hypothesis. Large (small) dots imply higher (lower) finite-size scaling quality.

Error bars have been omitted because systematic errors dominate, which we currently can not estimate.

Comparison with the 3-sphere

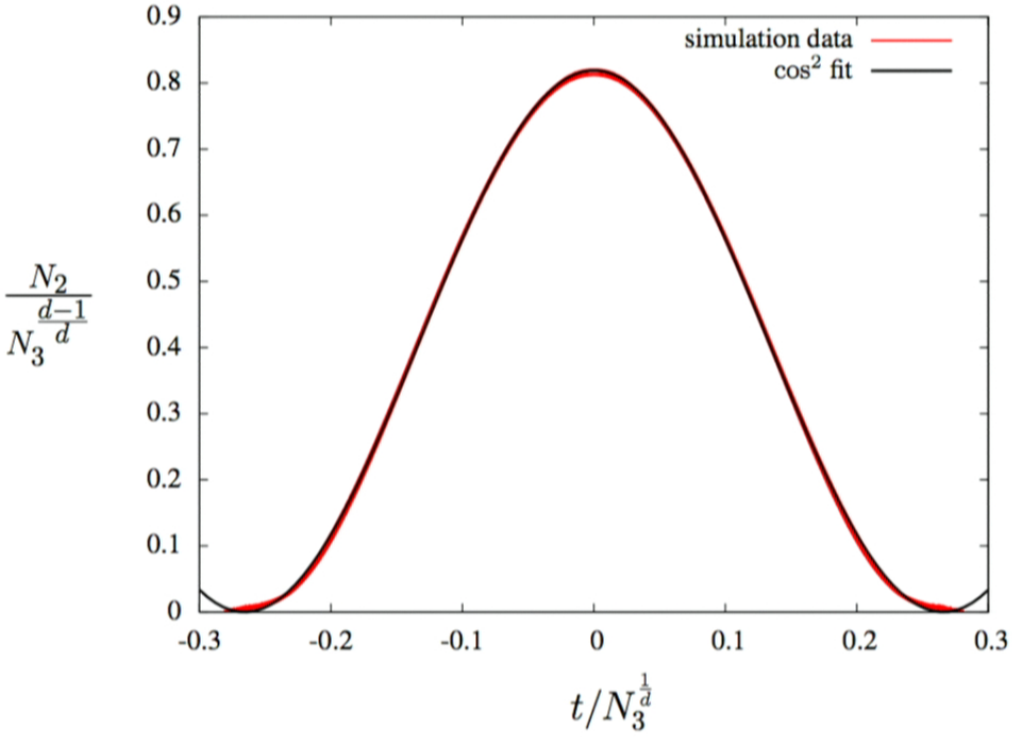

Here we fit the volume profile at $k = -0.8, \alpha = -1.0$ (far away from the CDT-corner) with the profile of a 3-sphere: $V_3(t) = a\cos^2(bt)$. The fit is almost perfect.

Summary

We have introduced a new model of dynamical triangulations with Lorentzian building blocks which does not have a preferred foliation.

Using a newly developed simulation software we have analyzed the dynamics of the model in 2+1 dimensions. The main results are:

- CDT emerges at the phase boundary at $\alpha = -0.5$.
- A phase of extended geometries containing "weakly foliated" triangulations.
- Strong evidence for $d = 3$ (global Hausdorff dimension).
- Excellent agreement of the volume profile with the profile of the 3-sphere (Euclidean de Sitter space in 2+1 dimensions).

Conclusions

CDT and the locally causal DT model appear to have a similar low-energy behavior in 2+1 dimensions (to be confirmed by measuring other observables).

There is a good chance that the same may be true for $d = 3 + 1$ as well.

If this is verified, having a preferred foliation appears to be a choice of convenience rather than a choice of necessity.

Outlook / ToDo

- Measure other observables such as the spectral dimension.
- Get a better handle on systematic errors.
- Solve the remaining technical problems (new Monte Carlo moves?).
- Solve the 1+1 dimensional model analytically (two Master projects so far, a solution is still not available).
- Analyze the 1+1 dimensional model numerically (ongoing Master project in Nijmegen).
- Analyze the 3+1 dimensional model numerically. A hard problem, is it feasible to be done at all?

Comparison with the 3-sphere

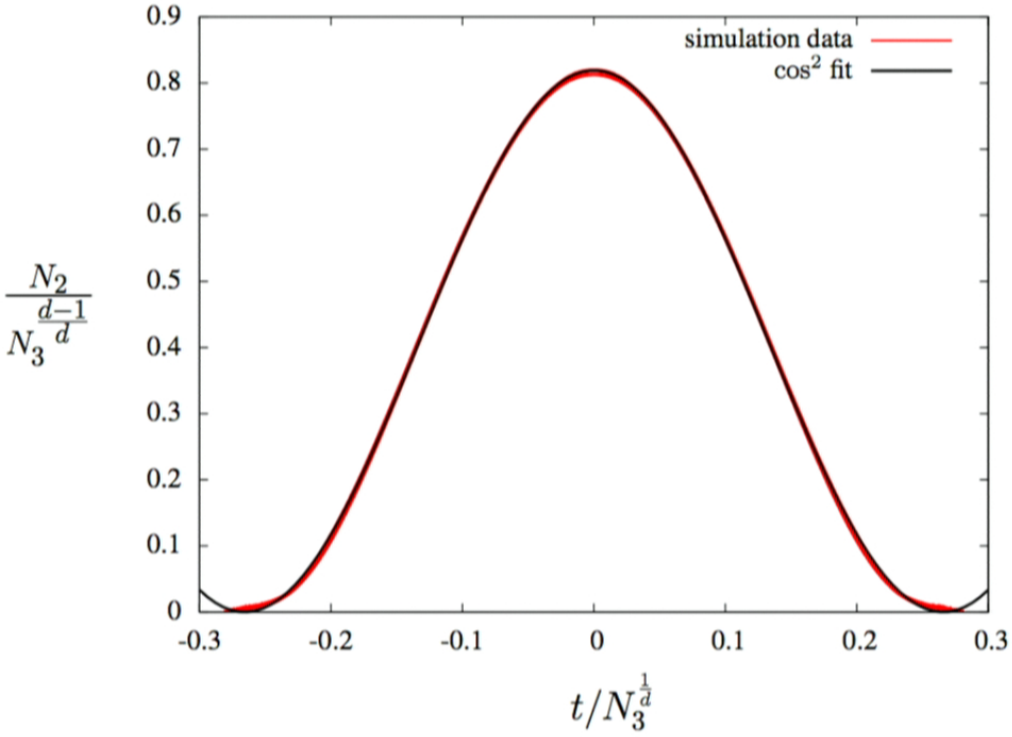

Here we fit the volume profile at $k = -0.8, \alpha = -1.0$ (far away from the CDT-corner) with the profile of a 3-sphere: $V_3(t) = a\cos^2(bt)$. The fit is almost perfect.

The regularized path integral

The CDT prescription allows us to convert the formal expression for the continuum path integral into a form which is suitable to be explored using Monte Carlo simulations:

$$Z(G_{\text{bare}}, \Lambda_{\text{bare}}) = \int_{\text{geometries}} \mathcal{D}[g] \exp(iS_{EH}[[g]])$$

$$\Downarrow$$

$$Z(\kappa_0, \kappa_4, \Delta) = \sum_{T \in \mathcal{T}} \frac{1}{C(T)} \exp(-S^{\text{eucl}}_{\text{Regge}}(T))$$

$\mathcal{T}$ is the space of all foliated triangulations and $1/C(T)$ is a discrete measure.